Journal of Catalysis **195,** 416–419 (2000)
doi:10.1006/jcat.2000.2997, available online at http://www.idealibrary.com on IDEAL®

RESEARCH NOTE

Adsorption and Photooxidation of Formamide on Powdered TiO_2

Wen-Chun Wu, Li-Fen Liao, Chih-Chung Chuang, and Jong-Liang Lin[1]

Department of Chemistry, National Cheng Kung University, 1, Ta Hsueh Road, Tainan, Taiwan 701, Republic of China

Received March 21, 2000; revised June 27, 2000; accepted July 14, 2000

Adsorption and photooxidation of formamide on TiO_2 have been studied by Fourier-transformed infrared spectroscopy. Formamide is adsorbed with intact molecular form ($HCONH_2$(a)) and dissociative form (η^2(N,O)-HCONH) on the surface at 35°C. They are subject to decomposition upon UV illumination in O_2. Adsorbed isocyanate (NCO) and formate (HCOO) and gaseous CO_2 and N_2O are formed in the photooxidation. CO_2 formation mainly results from NCO(a) photodecomposition. © 2000 Academic Press

Key Words: **formamide; TiO_2; adsorption; photooxidation; Fourier-transformed infrared spectroscopy.**

INTRODUCTION

Due to the unique electron density distribution of the formamide molecule, with localized electron lone pairs on the oxygen and nitrogen atoms as well as the carbonyl π bond, determination of the bonding geometry and reactivity of formamide on metal surfaces has been the subject of several molecular vibrational studies. Different surface bonding configurations, dependent on surface temperature, coverage, and preadsorbed atoms, have been proposed. On Ru(001) (1, 2), at low coverages formamide loses the hydrogen that attaches to the carbon atom at 80 K and adopts η^2(C,O)-NH_2CO bonding configuration, as evidenced by high-resolution electron energy-loss spectroscopy. At higher exposures, molecular formamide is adsorbed, interacting with the surface by the oxygen lone pair electrons at temperatures <80 K. On oxygen-preadsorbed Ru(001)–p(1 × 2)–O surface (3), formamide is adsorbed molecularly at low temperatures and decomposes to form η^2(N,O)-HCONH at 260 K. Higher temperatures cause further dissociation for the above surface species. On Ni(111) reflection absorption infrared spectroscopy shows two different reaction pathways to form HCO(a) and NH_2(a) at 235–260 K and to form HNCO(a) at 285 K (4). On Pt(111) formamide decomposes into NH_3 and CO at 170 K (5). Thermal reactions of formamide have also been studied on the supported systems of Pd/Al_2O_3 (6), Fe/Al_2O_3 (7), and Fe/SiO_2 (7) by infrared spectroscopy. Isocyanate species (NCO) are observed from formamide thermal dissociation on these surfaces.

TiO_2 has been extensively used recently as a photocatalyst to destroy environmentally detrimental molecules. To our knowledge, no interaction of formamide with TiO_2 has been reported. In the present paper, we investigate the adsorption and photooxidation of formamide adsorbed on TiO_2 by Fourier-transformed infrared spectroscopy. Due to its unique molecular structure, versatile photoreaction pathways are observed.

EXPERIMENTAL

The sample preparation of TiO_2 powder supported on a tungsten fine mesh (∼6 cm^2) has been described previously (8, 9). In brief, TiO_2 powder (Degussa P25, ∼50 m^2/g, anatase 70%, rutile 30%) was dispersed in a water/acetone solution to form a uniform mixture which was then sprayed onto a tungsten mesh. After that, the TiO_2 sample was mounted inside the IR cell for simultaneous photochemistry and FTIR spectroscopy. The IR cell with two CaF_2 windows for IR transmission down to 1000 cm^{-1} was connected to a gas manifold which was pumped by a 60 l/s turbomolecular pump with a base pressure of $\sim 1 \times 10^{-7}$ Torr. The TiO_2 sample in the cell was heated to 450°C under vacuum for 24 h by resistive heating. The temperature of TiO_2 sample was measured by a K-type thermocouple spot-welded on the tungsten mesh. Before each run of the experiment, the TiO_2 sample was heated to 450°C in vacuum for 2 h. After the heating, 10 Torr O_2 was introduced into the cell as the sample was cooled to 70°C. When the TiO_2 temperature reached 35°C, the cell was evacuated for gas dosing. O_2 (99.998%) was purchased from Matheson. Formamide (99.5%) from Aldrich was purified by several cycles of freeze–pump–thaw before introduction to the cell. Pressure was monitored with a Baratron capacitance manometer and an ion gauge. In the photochemistry study, both the UV and

---

[1] To whom correspondence should be addressed. Fax: 886-6-2740552. E-mail: jonglin@mail.ncku.edu.tw.

0021-9517/00 $35.00

IR beams were set 45° to the normal of the TiO_2 sample. The UV light source used was a combination of a Hg arc lamp (Oriel Corp.) operated at 200 W, a water filter, and a band pass filter with a band width of ~100 nm centered at 320 nm (Oriel 51650). Formamide is transparent for the UV wavelength used in the present study (10). The power at the position of the TiO_2 sample was ~0.1 W/cm^2 measured in the air by using a power meter (Molectron, PM10V1). Infrared spectra were obtained with a 4 cm^{-1} resolution by using a Bruker FTIR spectrometer with a MCT detector. The entire optical path was purged with CO_2-free dry air. The spectra presented here were ratioed against a clean TiO_2 spectrum. The mass of TiO_2 used was ~71 mg.

RESULTS AND DISCUSSION

Figure 1 shows the infrared spectra of formamide-adsorbed TiO_2 surface, which is prepared by exposing a clean TiO_2 surface at 35°C to formamide vapor for 20 min followed by evacuation, taken after the indicated times during the photooxidation course initially in 10 Torr of oxygen. Prior to UV irradiation, absorption bands are observed at 1310, 1355, 1382, 1568, 1590, 1675, 1698, 2861, 3170, 3263, 3335, and 3500 cm^{-1}. In 3600–3800 cm^{-1} region, absorptions from residual surface hydroxyl groups are attenuated, indicating the interaction, probably through hydrogen bonding, between surface hydroxyl and adsorbed species. By examination of the infrared absorptions and band assignment of formamide in liquid and solid states as shown in the second and third columns of Table 1, some of the bands observed after formamide adsorption on TiO_2 can be related to the functional absorptions of NH_x, CH, C=O, and C–N. Table 1 also shows the infrared bands and their vibrational assignments for formamide molecules adsorbed on various surfaces. In accordance with these previous studies, we conclude the formation of adsorbed formamide on TiO_2 in our case and assign the band at 1310 cm^{-1} to C–N stretch, 1382 cm^{-1} to CH deformation, 1590 cm^{-1} to NH_2 deformation, 1675 and 1698 cm^{-1} to carbonyl stretch, 2861 cm^{-1} to CH stretch, and 3160 and 3500 cm^{-1} to NH stretch, as listed in the last column of Table 1. In addition to the NH_2 stretching, the broad absorption feature at 3050–3550 cm^{-1} may also be due to overtone absorption of C=O stretch, NH_2 deformation, and hydrogen bonding. The carbonyl frequencies of adsorbed formamide are generally lower than that of the gaseous one. This may be due to the interaction between the adsorbed formamide molecules, as suggested by the lower carbonyl frequency observed in the liquid formamide molecules, and/or due to the interaction of the carbonyl group of formamide with surfaces. The other two strong bands at 1355 and 1568 cm^{-1} do not belong to adsorbed formamide on TiO_2. On Ru(001)–p(1 × 2)–O (3) and Pd/Al_2O_3 (6) surfaces, except for the molecularly

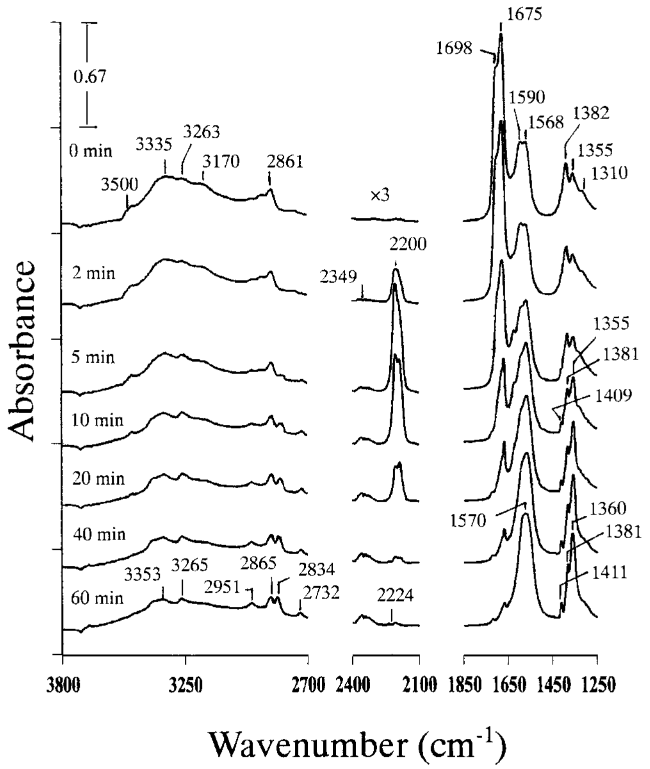

FIG. 1. Variation of infrared spectra with UV irradiation time for a TiO_2 surface after formamide adsorption. The curves at 2100–2400 cm^{-1} have been multiplied by a factor of 3.

TABLE 1

Comparison of Vibrational Frequencies (cm^{-1}) of Formamide Adsorbed on Various Surfaces

	Gas (Refs. 11, 12)	Liquid (Ref. 13)	Pd/Al_2O_3 (Ref. 6)	Ru(001)–p(1 × 2)–O (Ref. 3)	Ni(111) (Ref. 4)	Pt(111) (Ref. 5)	TiO_2 (this work)
ν_a (NH_2)	3545	3330	—	3490	3348	3289	3500
ν_s (NH_2)	3451	3190	—	3230	3132	3145	3170
ν (CH)	2852	2882	—	2940	2865	2834	2861
ν (CO)	1734	1690	1684	1660	1706	1685	1675, 1698
δ (NH_2)	1572	1608	1600	1585	1602	1593	1590
δ (CH)	1378	1391	1385	—	1385	—	1382
ν (CN)	1255	1309	1315	1360	1293	1291	1310

TABLE 2

Comparison of Vibrational Frequencies (cm^{-1}) of η^2(N,O)-HCONH

	Ru(001)–p(1 × 2)–O (Ref. 3)	Pd/Al_2O_3 (Ref. 6)	Al_2O_3 (Ref. 14)	TiO_2 (this work)	$[R_2MN(CH_3)C(CH_3)O]_2$ (Ref. 15)
ν (NH)	3365				
ν (CH)	2980				
ν_a (NCO)	—	1600	1600	1568	1571–1585
ν_s (NCO)	1395	1360	1375	1355	1392–1400

adsorbed formamide, bridging bonding configuration of η^2(N,O)-HCONH from N–H bond scission after formamide adsorption has been identified. η^2(N,O)-HCONH is also formed by the interaction of HCN with surface hydroxyl groups on Al_2O_3 (14). Therefore, with absorption frequencies of 1355 and 1568 cm^{-1} observed in the present study similar to those of η^2(N,O)-HCONH on Ru(001)–p(1 × 2)–O (3), Pd/Al_2O_3 (6), and Al_2O_3 (14) as well as in organometallic compounds as shown in Table 2, it is concluded that bridging η^2(N,O)-HCONH is formed following formamide adsorption on TiO_2 at 35°C and the bands of 1355 and 1568 cm^{-1} are due to –NCO– stretching. Analogous to formamide, formic acid forms bridging formate η^2(O,O)-HCOO on the TiO_2 surface with $-CO_2-$ symmetric and antisymmetric stretches at ∼1360 and ∼1560 cm^{-1}, respectively (16, 17).

Upon UV irradiation, $HCONH_2$(a) and HCONH(a) undergo decomposition as evidenced by the decrease of their band intensity and formation of new bands in Fig. 1. Two new bands appear at 2200 and 2349 cm^{-1} after 2 min of irradiation. The band at 2349 cm^{-1} is due to CO_2(g) formation. The 2200 cm^{-1} band is due to isocyanate species, NCO(a), adsorbed on the surface. NCO(a) has been observed on Rh, Ru, Pt, and Pd surfaces with a frequency at ∼2170 cm^{-1} (18–20). NCO(a) can be produced with absorptions at 2170 and 2262 cm^{-1} by thermally activating formamide on Pd/Al_2O_3 (6), at 2220 and 2320 cm^{-1}on Fe/Al_2O_3 (7), and at 2200 and 2270 cm^{-1} on Fe/Al_2O_3 (7). Recently NCO(a) was identified at 2205 cm^{-1} in a photochemistry study of CH_3CN on TiO_2 (21). Upon further irradiation to 5 min, CO_2(g) and NCO(a) grow with UV time and the peak shape at 1250–1850 cm^{-1} is slightly changed. After 10 min, absorptions peak at 1355, 1381, and 1409 cm^{-1} in the 1250–1450 cm^{-1} range and the intensity ratio of 1355 cm^{-1} relative to 1381 cm^{-1} is opposite to that of 1355 cm^{-1} relative to 1382 cm^{-1} before UV irradiation. UV irradiation for 20 min causes the reduction of the new band at 2200 cm^{-1}. After 60 min, $HCONH_2$(a) and HCONH(a) are substantially reduced and absorption bands appear at 1360, 1381, 1411, 1570, 2732, 2834, 2865, 2951, 2224, and 2349 cm^{-1}. The 2224 cm^{-1} band is due to formation of N_2O(g) which is also observed as a product in the photooxidation of ammonia on TiO_2 (22, 23). The first eight bands can be attributed to adsorbed formate groups, which have been detected after adsorption of formic acid (16) or formaldehyde (17) on TiO_2. The 1360 and 1570 cm^{-1} bands are due to $-CO_2-$ symmetric and antisymmetric stretching, respectively, and the 1381 and 1411 cm^{-1} bands are due to C–H deformation or $-CO_2-$ rocking. The other four bands at 2732, 2834, 2865, and 2951 cm^{-1} are due to CH stretch and combination of CH deformation and $-CO_2-$ stretch.

The following reaction scheme summarizes the intermediates and products formed in the photooxidation of formamide on TiO_2:

$$\begin{aligned} \mathrm{HCONH_2(a), HCONH(a)} &\rightarrow \mathrm{NCO(a) + HCOO(a)} \\ &\rightarrow \mathrm{CO_2(g)} \rightarrow \mathrm{N_2O(g)}. \end{aligned}$$

For the formation of NCO(a), breaking of H–C and N–H bonds must occur in the photooxidation of $HCONH_2$(a) and/or HCONH(a). For HCOO(a) from $HCONH_2$(a) and/or HCONH(a), scission of the C–N bond is necessary. Once NH_2 or NH is formed, N_2O(g) is derived from them in subsequent photooxidation as in the case of NH_3 on TiO_2 (22, 23). N_2O(g) may also be produced from photooxidation of the NCO(a) intermediate. CO_2(g) can be formed in the photodecomposition of HCOO(a) and NCO(a) (20). Under our experimental conditions, ∼90% of the total CO_2 amount is formed during the first 20 min during which substantial NCO(a) is present on the surface and only ∼5% is formed in the last 20 min during which the surface is dominated by HCOO(a). Therefore, CO_2 mainly originates from NCO(a) photooxidation in the present study. It should be pointed out that the TiO_2 temperature was raised to 57°C during the formamide photooxidation process. Therefore, a thermal control experiment was carried out by holding the formamide-adsorbed TiO_2 at 57°C in 10 Torr of O_2 for 60 min and taking the infrared measurement during the annealing. Figure 2 shows the results. The spectrum after 60 min of annealing, except for the decrease of the $HCONH_2$(a) bands, is similar to that before surface heating. No reaction intermediates and products are observed, indicating that the reaction induced by the UV irradiation is due to photon, instead of thermal effect. In the production of NCO(a) in the present study, it is of interest to determine whether the O in the NCO(a) originates from formamide itself, TiO_2 lattice oxygen, or O_2. Therefore, photooxidation of formamide in the presence of $^{18}O_2$ has been carried out. It is found that in this experiment the infrared absorption frequency of isocyanate formed from formamide photodegradation is the same as that in Fig. 1 when $^{16}O_2$ is used. If $NC^{18}O$(a) were produced, it would absorb at a frequency lower than that of $NC^{16}O$(a) absorption by ∼13 cm^{-1} (21). However, no such a red-shifted peak is observed, indicating that the O in the NCO(a) is not from O_2. Besides, when $^{18}O_2$ is present, it can be dissociatively adsorbed or be

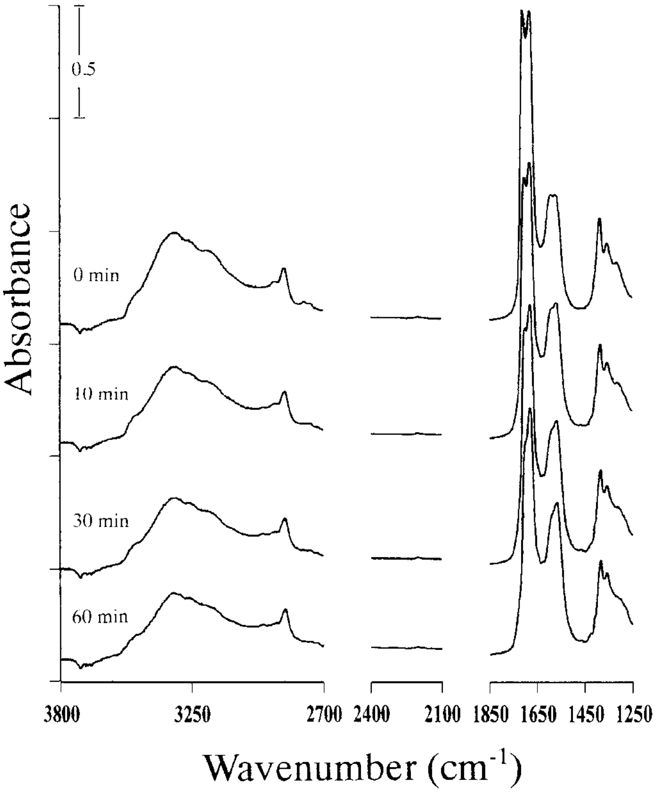

FIG. 2. Variation of infrared spectra with annealing time at 57°C for a TiO_2 surface after formamide adsorption.

photochemically dissociated at O-lattice vacancy sites present on powdered TiO_2 (21). The lack of $NC^{18}O(a)$ production also suggests that the O of the NCO(a) dose not result from TiO_2 lattice oxygen.

Many organic molecules can be effectively photooxidized on TiO_2 with UV illumination. As TiO_2 accepts photons with energy higher than its bandgap (3.2 eV), electron–hole pairs can be produced and migrate to the surface where they initiate redox reactions of adsorbates. $OH^\bullet$ radicals, possibly from the reaction of surface hydroxyl groups or water with holes, have been proposed to be the oxidizing agent. Identification of OH adducts (24–27) and studies of kinetic isotopic effect (28) support this mechanism. There is also evidence for direct hole oxidation. Draper and Fox (29) have not been able to detect any $OH^\bullet$ adduct intermediates in the diffuse reflectance flash photolysis study of several substrate/TiO_2 combinations. Adsorbed O_2 can trap electrons to form O_2^- and therefore increase the lifetime of hole states. In the previous studies of the interaction of O_2 with the TiO_2 surface upon UV irradiation, EPS has shown the existence of O_2^-, O_3^-, and O_2^{3-} (30), which can behave as oxidants. The initiating mechanism of photooxidation for adsorbates on TiO_2 is still under discussion.

ACKNOWLEDGMENTS

We gratefully acknowledge the financial support of the National Science Council of the Republic of China (Grant NSC 89-2113-M-006-008) for this research.

REFERENCES

1. Parmeter, J. E., Schwalke, U., and Weinberg, W. H., *J. Am. Chem. Soc.* **109**, 1876 (1987).
2. Parmeter, J. E., Schwalke, U., and Weinberg, W. H., *J. Am. Chem. Soc.* **110**, 53 (1988).
3. Parmeter, J. E., Schwalke, U., and Weinberg, W. H., *J. Am. Chem. Soc.* **109**, 5083 (1987).
4. Gao, Q., Erley, W., Sander, D., Ibach, H., and Hemminger, J. C., *J. Phys. Chem.* **95**, 205 (1991).
5. Flores, C. R., Gao, Q., and Hemminger, J. C., *Surf. Sci.* **239**, 156 (1990).
6. Paul, D. K., and Worley, S. D., *J. Phys. Chem.* **94**, 8956 (1990).
7. Johnston, C., Jorgensen, N., and Rochester, C. H., *J. Chem. Soc., Faraday Trans. 1* **85**, 1111 (1989).
8. Basu, P., Ballinger, T. H., and Yates, J. T., Jr., *Rev. Sci. Instrum.* **59**, 1321 (1988).
9. Wong, J. C. S., Linsebigler, A., Lu, G., Fan, J., and Yates, J. T., Jr., *J. Phys. Chem.* **99**, 335 (1995).
10. Calvert, J. G., and Pitts, J. N., Jr., "Photochemistry." Wiley, New York, 1996.
11. Evans, J. C., *J. Chem. Phys.* **22**, 1228 (1954).
12. King, S. T., *J. Phys. Chem.* **75**, 405 (1971).
13. Suzuki, I., *Bull. Chem. Soc. Jpn.* **33**, 1359 (1960).
14. Krietenbrink, H., and Knözinger, H., *Z. Phys. Chem.* **102**, 43 (1976).
15. Schwering, H. U., and Weidlein, J., *Chimia* **27**, 535 (1973).
16. Chuang, C.-C., Wu, W.-C., Huang, M.-C., Huang, I.-C., and Lin, J.-L., *J. Catal.* **185**, 423 (1999).
17. Busca, G., Lamotte, J., Lavalley, J.-C., and Lorenzelli, V., *J. Am. Chem. Soc.* **109**, 5197 (1987).
18. Solymosi, F., Völgyesi, L., and Raskó, J., *Z. Phys. Chem.* **120**, 79 (1980).
19. Solymosi, F., Völgyesi, L., and Sárkány, J., *J. Catal.* **54**, 336 (1978).
20. Solymosi, F., Sárkány, J., and Schauer, A., *J. Catal.* **46**, 297 (1977).
21. Zhuang, J., Rusu, C. N., and Yates, J. T., Jr., *J. Phys. Chem.* **103**, 6957 (1999).
22. Mozzanega, H., Herrmann, J.-M., and Pichat, P., *J. Phys. Chem.* **83**, 2551 (1979).
23. Cant, N. W., and Cole, J. R., *J. Catal.* **134**, 317 (1992).
24. Milles, G., and Hoffman, M. R., *Environ. Sci. Technol.* **27**, 1681 (1993).
25. Wei, T. Y., and Wan, C., *J. Photochem. Photobiol. A* **69**, 241 (1992).
26. Mills, A., Morris, S., and Davies, R., *J. Photochem. Photobiol. A* **70**, 183 (1993).
27. Goldstein, S., Czapski, G., and Rabani, J., *J. Phys. Chem.* **98**, 6586 (1994).
28. Cunningham, J., and Srijarana, S., *J. Photochem. Photobiol. A* **43**, 329 (1998).
29. Draper, R. B., and Fox, M. A., *Langmuir* **6**, 1396 (1990).
30. Meriaudeau, P., and Vedrine, J. C., *J. Chem. Soc., Faraday Trans. 2* **72**, 472 (1976).